2019

Coupled Numerical Analysis of Variations in the Capacity of Driven Energy Piles in Clay

Arvin Farid
Boise State University

Daniel P. Zimmerman
Boise State University

Coupled Numerical Analysis of Variations in the Capacity of Driven Energy Piles in Clay

Arvin Farid, Ph.D., P.E., M.ASCE, [1] and Daniel P. Zimmerman, [2]

[1]Associate Professor, Department of Civil Engineering, Boise State University, 1910 University Dr., MS. 2060, Boise, ID 83725-2060; e-mail: arvinfarid@boisestate.edu

[2]Graduate Student, Department of Civil Engineering, Boise State University, 1910 University Dr., MS. 2060, Boise, ID 83725-2060; danielzimmerman@u.boisestate.edu

ABSTRACT

Energy piles are an emerging alternative for the reduction of energy consumption used to heat and cool buildings. Most of the research to date has been on thermodynamic properties or axial and radial stress and strain of piles. This paper focuses on the temperature-fluctuation effect on the capacity of vertically loaded driven energy piles in clayey soils. Consolidation of clay surrounding driven piles affects the pile capacity (i.e., set up in clay). The heating and cooling periods of energy piles can create the excess pore-water pressure (EPWP, u_e) or relax the existing one (e.g., due to pile driving or previous thermal loads) in clayey soils (due to the contraction and expansion of water) affecting the pile capacity. In the meantime, the thermal expansion and contraction of the pile also generate or relax the EPWP in the soil, which can be computed using the cavity-expansion theory. This paper studies the resulting changes in the pile capacity due to the daily and seasonal thermal cycles. The results show that thermal cycles in an energy pile can cause a decrease in the pile capacity leading to a delay in reaching the capacity after a complete clay set up.

INTRODUCTION

Energy piles are an emerging alternative for the reduction of fossil-fuel energy consumption to heat and cool buildings. Energy piles combine ground-sourced heating and cooling systems with the building's foundation. In recent history, heat exchange within the soil had been accomplished by horizontal heating and cooling beds, or heat sinks outside of the building footprint. The use of ground-source heat pumps (GSHPs) requires additional ground surface outside of the building footprint (Brandl, 2006). This requirement eliminates their use in most urban settings. While GSHPs require less energy to heat and cool structures, they have not been widely used in the United States due to higher installation costs than conventional heating and cooling methods (McCartney and Rosenberg, 2011). Energy piles have advantages over separate foundation and GSHP systems, including lower installation costs and no requirement for additional space. Energy piles serve the dual purpose of supporting the structure and serving as a heat exchange medium. Energy piles have been installed in Austria and Switzerland for the last 30 years and are gaining popularity in other parts of Europe (Brandl, 2009). Energy piles have not yet been

embraced by other developed countries more than the United States, mainly due to insufficient research concerning the effects of temperature fluctuation on the stress state of the foundation soils (McCartney and Rosenberg, 2011), initial construction cost, and the lack of U.S. requirements to utilize green energies in buildings, which is more common in Europe.

The adverse effect from energy piles may arise from the cyclic thermal loading of soils. In other words, the cyclic temperature change results in cyclic loading, which may potentially result in a reduction of the pile capacity. The cyclic thermal loading in fine-grained soils can affect the shear strength of soil since shear strength can be temperature-dependent. However, in fine-grained soils such as clay, in addition to the temperature-dependent shear strength, the thermal cyclic loading can cause cyclic variations of the excess pore-water pressure (EPWP, u_e). Cyclic variations of the EPWP cause cyclic variation of the effective stress, and the shear strength and volume changes triggered by the temperature cycles can reach a state of thermo-elasticity after the first few cycles. The focus of this paper is on the latter effect.

SCOPE AND METHODOLOGY

Model

This paper uses the finite-difference method to analyze the impact of thermal cycles in an energy pile located within the clay. A coupled numerical model has been developed using principles of three-dimensional (3D, axisymmetric (radial) and vertical) primary consolidation of, and heat transfer through, saturated, slightly over-consolidated clay around a driven circular energy pile. The driving effect is captured through an increase in excess pore-water pressure (u_e) and lateral stress modeled using the cavity expansion theory. The increase/decrease of u_e due to temperature variations in clay and the expansion or contraction of the pile were modeled and analyzed.

Modeling Material Properties and Pile Capacity

The temperature of the soil surface adjacent to the energy pile was varied to simulate seasonal heating and cooling demands. For the purpose of this paper, temperature changes adjacent to the pile were assumed on the order of 52 °C (- 1 °C to + 51 °C) between peak heating and peak cooling temperatures; however, temperature change estimated for energy piles in the U.S. are in the ±15°C range (Abdelaziz, 2016). The model simulated the 3D dissipation of the u_e through the clay surrounding the pile. The resulting temporal variations of the pile capacity due to this cycling were computed. Thermal conductivity coefficients and specific heat capacities for the soil matrix were estimated using accepted values for soil and water found in the literature (Campanella and Mitchell, 1968). Coefficients of thermal expansion for the concrete piles, soil, and water were also assigned to the model according to accepted values found in the literature (Campanella and Mitchell, 1968). A driven energy pile that was modeled over a 2.5-year period with a constant-surface-temperature boundary condition and a transient-surface-temperature boundary condition assumed to be ($T = T_{med} + \left(\frac{T_h - T_l}{2}\right) * \cos\left[\frac{2\pi(t-212)}{364}\right]$ where time, t, is in days.

The purpose of the transient-surface temperature iteration is to simulate an energy pile that is near an exterior wall that may be subjected to seasonal temperature changes of the ground surface. Summary of results and conclusions will be discussed in the following.

The soil was modeled as a homogeneous layer of anisotropic clay for vertical and radial permeabilities. The study consists of three related, but stand-alone, models. Two of the models analyze a driven energy pile. One of these models includes transient ground-surface temperatures, and one assumes a constant surface soil temperature. Both of these driven-pile models assume the pile is driven six months before the HVAC system is turned on.

The soil was modeled as a saturated, slightly over-consolidated clay of medium to high plasticity. The characteristics of the clay were similar to the Illite tested by Campanella and Mitchell (1968) as shown in Table 1.

Table 1. Properties of clay at 20 ºC Campanella and Mitchell (1968)

α_s	c_p	K	k_{rr}	k_{zz}	γ_{sat}	e_0
3.3 $\times 10^{-7}$ /°C	2,462 J/kg.°C	.0042 W/m/ºK	7 $\times 10^{-7}$ m/s	4 $\times 10^{-7}$ m/s	17 kN/m^3	1.1

E_s	G_s	υ_s	s_u	φ'	OCR	PL	LL
20 MPa	2.75	0.3	75 kPa	20º	1.1	17	52

where e_0 was the initial void ratio; k_{rr} is the horizontal (radial) hydraulic conductivity; k_{zz} was the vertical hydraulic conductivity; γ_{sat} was the void ration was readjusted by the model as a result of the cavity expansion due to pile driving and soil expansion and contraction. The saturated unit weight were adjusted as the void ratio after the pile was driven or after soil expansion or contraction., , but it is E_s was the Young's modulus for the soil; G_s was the specific gravity of the soil,; υ was the Poisson's ratio of the soil; s_u was the undrained shear strength of the clayey soil, ; φ' was the angle of effective internal friction of the clay; OCR was the over-consolidation ratio; and LL and PL were the liquid and plastic limits respectively.

K was the heat conductivity coefficient for both vertical and radial directions; α_s was the coefficient of thermal expansion for the saturated soil 3.3 $\times 10^{-7}$ /°C; c_p was the specific heat for the clay, c_p, is at 20 °C, and the physicochemical coefficient of structural volume change is -0.5 $\times 10^{-4}$ /°C after Campanella and Mitchell (1968).

The thermal expansion of the pile in the radial direction was calculated using the equation for the thermal expansion of an area, $\Delta A = 2\alpha_T A_0 \Delta T$ where ΔA is the change in the area, A_0 is the original area, α_T is the coefficient of linear thermal expansion, and ΔT is the change in temperature. The new radius, R_1, may be calculated based on the initial radius, R, as $R_1 = [R^2 \times (1 + 2\alpha_T \Delta T)]^{0.5}$.

The coefficient of thermal expansion, α_{pile}, of the concrete for the driven pile was assumed 14.5 $\times 10^{-6}$ /°C. The Young's Modulus for the concrete was assumed 25 MN/m^2. The coefficient of

thermal expansion for water, α_{H2O}, was set to 0.207 ×10^{-3} /°C. Water density, ρ_w, is 999.973 kg/m^3 at 4 °C but was continually recalculated based upon the current temperature within the model. Dynamic viscosity is the measure of a fluid's resistance to deformation by shear or tensile stresses.

The Vogel-Fulcher-Tammann (VFT) model for dynamic viscosity, μ, was used to find values for the variation of the dynamic viscosity of water with temperature (Trachenko, 2008). The general form of the VFT model is as follows. Abdelaziz (2013) performed a sensitivity analysis that showed no significant impact of the minor change in the fluid properties on the thermal and mechanical response of energy piles. This is because the temperature range is small enough.

$$\mu = e^{\left(A+\frac{B}{C+T}\right)} \quad (\mathbf{1})$$

where T is the temperature in ^{o}K; and coefficients A, B, and C for water were obtained from VFT-equation viscosity calculator for a variety of fluids. The VFT equation for the dynamic viscosity of water, with coefficients, is hence as follows.

$$\mu = e^{\left(-3.7188+\frac{578.919}{-137.546+T^{oK}}\right)} \quad (\mathbf{2})$$

Because of the hydraulic conductivity changes when the temperature changes, it is adjusted continuously within the model as follows.

$$k_T = K\frac{\gamma_T}{\mu_T} = \left(k_{20^\circ C}\frac{\mu_{20^\circ C}}{\gamma_{20^\circ C}}\right)\frac{\gamma_T}{\mu_T} \quad (\mathbf{3})$$

where γ is the unit weight of the permeant fluid (here water), and μ is the dynamic viscosity of the permeant fluid (here water). The subscripts represent the temperature in ^{o}C (Holtz et al., 2011). Equation (3) inherently assumes that the change in the K depends only on the change of the viscosity. In other words, it does not consider changes in the microstructure of the soil (e.g., pore sizes and connectivity)

The coefficient of volumetric compressibility for water, m_v, was set at -0.364 ×10^{-3} m^2/kg. The coefficient of compressibility was selected so the u_e dissipation would complete within 910 days such that the clay modeled in this work would have physical characteristics similar to the Illite studied Campanella and Mitchell (1968). Consolidation was set to update on a daily basis within the model. The initial temperature of the soil was set to 15 °C (288 ^{o}K).

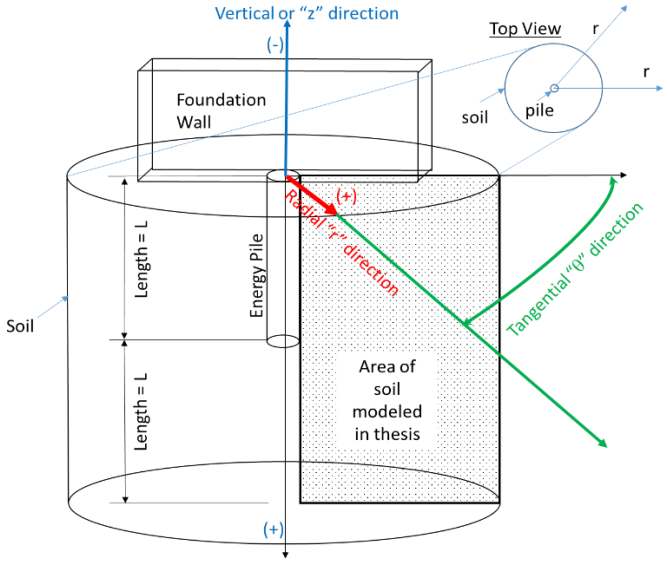

Figure 1. The layout of the model energy pile and simulated soil in cylindrical coordinates. Temperatures fluctuate between - 1 °C and + 51 °C in the soil adjacent to the energy pile.

The axisymmetric finite-difference mesh used to model the soil is a rectangular grid of 21 nodes wide and 31 nodes high, for a total of 651 nodes, as shown in Figure 1. The width of the mesh was modeled at approximately 3.33 m (at increments of dr = 0.167 m), and the height of the mesh was modeled at 30 m (at increments of dz = 1 m). The driven pile was represented as a boundary condition from the top left corner of the mesh to mid-height. The pile was assumed to be 15 m long. The boundary condition below the pile to the bottom left corner is soil, assumed to be symmetrical to the soil below the pile. The bottom row of the mesh was modeled to be impermeable since the modeled soil was clay (and could be modeled symmetrical if the model soil were sand). This selection was made based upon the hydraulic conductivity of the soil. The top of the mesh was assumed to have a concrete cover or pile cap over the half of the surface near the pile. The other half of the top of the mesh was assumed to be exposed to the air.

The driven-pile model assumes that the structure built upon the energy piles will be built and operational, at least from the standpoint of HVAC system operation, exactly six months after pile installation. The modeled pile is representative of a typical pile, and no distinction is made between an interior pile and exterior (or perimeter) pile, except for the transient ground-surface temperature iteration of the model, which may be interpreted for an exterior pile. Consideration of the specifics of the construction of the building's foundation (within the pile) are beyond the scope of the model.

The model establishes a period through the initial six-month period prior to HVAC introduction, which allows for dissipation of u_e and consolidation of the modeled soil. Both versions of the driven-pile model also calculate u_e dissipation for a period of two years plus six months, or 910 days, without HVAC system introduction, so that consolidation without conduction may be compared to consolidation with conduction.

As the six-month period begins within the time loop, the density and coefficient of thermal expansion of the water are calculated based upon the in-situ temperature. Next, the physical state

of the soil is changed due to pile driving. The initial void ratio, e_0, is recalculated to in-situ values using Equation (4) for an element of unit length. In Equation (4), C_c is the compression index; K_o is the at-rest lateral earth-pressure coefficient; and γ_{sat} is the initial saturated unit weight.

$$e_1 = e_0 - C_c[\log_{10}(K_o.\gamma_{sat}.z) - \log_{10}(K_o\gamma_{sat}.(1))] \quad (\mathbf{4})$$

The installation of the pile will increase the radial stress based on Equation (5). Equation (5) utilizes site-specific factors and restrike data, that is, data obtained from driving the pile ssometimesafter driving has initially ceased, whether a few hours or several days. Re-striking is performed to either determine the capacity of the pile or to try to obtain additional penetration (Ng et al., 2013).

$$\frac{Q}{Q_0} = A\log_{10}\left(\frac{t}{t_0}\right) + 1 \quad (\mathbf{5})$$

where Q is the capacity of the pile at time = t; Q_0 is the capacity of the pile at time = t_0, which is the time at which the dissipation of u_e becomes linear with the log of time (Steward and Wang, 2011). The setup factor, *A*, is dimensionless and varies depending on soil conditions and the type of the pile (Steward and Wang, 2011). The setup factor can range from 0.2 to greater than 1, where $A = 0.6$ is typically used for clay, and t_0 is typically valued at one day (Yang and Liang, 2006). However, the Skov and Denver equation is not used to predict ultimate pile capacity. The Skov and Denver equation assumes a linear increase in pile capacity, and since pile capacity does not increase to infinity, it is only valid for a limited time after pile installation (Wang et al., 2010).

As seen in the flowchart of Figure 2, a subroutine within the code recalculates the void ratio within the plastic zone based upon the increase in the stress. Once the void ratio and porosity are recalculated, γ_{sat} is also recalculated. After the density of water is calculated based upon the temperature, its dynamic viscosity is calculated according to Equation (2), and the absolute hydraulic conductivity is calculated according to Equation (3). Therefore, Darcy's assumptions were violated so that the changes in the permeability due to temperature changes could be examined in the model. The next values to be calculated by the model were the radial and vertical coefficients of consolidation, c_{rr} and c_{zz}, respectively. This calculation was performed using Equation (6), and the unit of c_{rr} was converted to days.

$$c_{rr} = \frac{k_{rr}(86{,}400\ sec/day)}{m_v\rho_w g} \quad (\mathbf{6})$$

The $\boldsymbol{u_e}$ is then calculated. The boundary condition along the pile face is calculated using the logarithmic decay of Equation (7) fitted to Bograd & Matlock (1996) and Banerjee (1978) models (Mirza, 2000). Once the value of u_e in Equation (7) reaches zero, the model limits the value of this boundary u_e to zero for cavity expansion.

$$u_e = 4.5 \cdot c_u\left[1 - \frac{\ln\left(\frac{c_r t}{R^2}\right)}{6}\right] \quad (\mathbf{7})$$

where *t* is time; and R is the lateral drainage path. Finally, the unit skin-friction resistance is calculated according to Equation (8).

$$f_s = \beta \sigma_z' \quad (\mathbf{8})$$

where $\beta = K_0 \left(\frac{K}{K_0}\right) \tan\left[\varphi' \left(\frac{\delta}{\varphi'}\right)\right]$ where φ' is the effective stress friction angle, and δ is the soil-foundation friction angle. The effective vertical stress, σ_z', is calculated for each one-meter thickness of soil using Equation (9). In Equation (9), for the calculation of unit friction for a 1m thick slice of soil at a depth of *x* m to a depth of *(x+1)* m, the value of the effective vertical stress is the overburden due to the above *(x)* m plus the effective vertical stress at the midpoint between *(x)* m and *(x+1)* m.

$$\sigma_z' = \gamma_{sat} \cdot (z-1) + 0.5(\gamma_{sat} - \rho_w \cdot g) \quad (\mathbf{9})$$

where

$$K_0 = (1 - \sin\varphi')OCR^{\sin\varphi'} \quad (\mathbf{10})$$

where

$$\mathrm{K} = 1.5 \cdot K_0 \quad (\mathbf{11})$$

$\left(\frac{K}{K_0}\right)$ values for a large displacement, driven pile range from 1.0 to 2.0 (Coduto, 2001). Values for the $\left(\frac{\delta\prime}{\varphi'}\right)$ ratio are given at 0.8 to 1.0 for smooth concrete, such as the one seen in a precast pile, and 1.0 for rough concrete (Coduto, 2001). In the model, $\left(\frac{K}{K_0}\right)$ is calculated using Equations (10) and (11), where φ' is 20°. The ratio $\left(\frac{\delta\prime}{\varphi'}\right)$ is assumed to be equal to 0.8 in the model. Unit-circumference-friction is calculated using a ratio of u_e to initial u_{e0}, with the assumption that u_{e0} at Day 1 is equal to 1.25 times the deviator stress, $\delta\sigma_r$, as shown in Equation (12). The unit friction calculated using Equation (8) equals the friction along a unit length of the pile. Because the model calculates friction along the entire effective length of the pile, the frictional capacity calculation only requires multiplying the results by the perimeter of the pile. Therefore, the friction value computed by the model will, here on, be referred to as the unit-circumference friction value.

$$f = \left(\sum K_0.\sigma_{z(ii)}' \cdot \frac{K}{K_0} \cdot \tan\left[\varphi'\left(\frac{\delta}{\varphi'}\right)\right]\right) * \left\{0.2 + 0.8\left[1 - \left(\frac{u_{e(ii)}}{\left(\frac{\delta\sigma_r}{0.8}\right)}\right)\right]\right\} \quad (\mathbf{12})$$

After the six-month construction period, all three versions of the model loop through two years of simulated seasonal heating and cooling cycles. The heating and cooling cycles are cyclical in nature and separated into thirteen-week seasons. The details of this portion of the model are presented below in Figure 2.

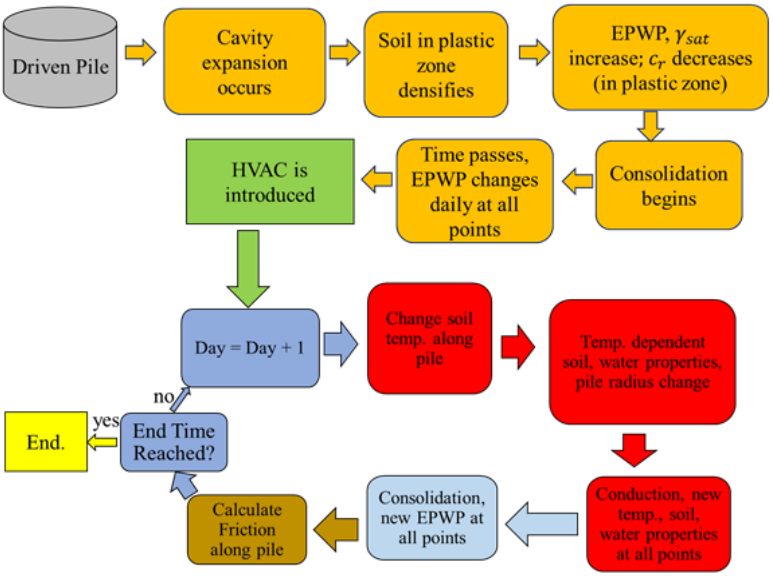

Figure 2. The process followed by the model for the driven-pile iterations.

After the initial six months, the u_e values are augmented by heat generated from the HVAC system. The HVAC system begins adding heat at the pile surface on the first day of summer. Heating of the energy pile through the convection of the heat carrying fluid within the pile, as described by Brandl (2009), is beyond the scope of this paper. Researchers such as Laloui et al. (2006) and Brandl (2009) present heating and cooling cycles that reach their maximum differential in a matter of days. The heat energy was added to and removed from the soil gradually in this model. In order to keep the quantity of heat added to the soil out of the model, a method of representing the gradual change in heat energy was devised. This gradual change in heat energy introduced or removed from the soil is represented in a gradual change in surface temperature of the soil adjacent to the energy pile. In addition, the gradual nature of the temperature change along the pile is meant to simulate the change in demand of the occupants of the theoretical building on the HVAC system throughout the calendar year. In the model, the highest demand on the cooling system would occur when the outside temperature was hottest. This time period is modeled to be in the middle of the summer season. Cooling of the building would pull heat from the occupied space and transfer that heat into the soil via the energy piles. This would then heat the soil. Conversely, the highest demand for heat would occur in the middle of the winter season, requiring the greatest amount of heat to be removed from the soil. The change between the demand for cooling and heating the building occurs gradually and linearly, with a week in the middle of autumn and another in the middle of spring where neither heating nor cooling is required for the building. The seasons are simulated as shown in Figure 3. Abdelaziz et al. (2014) present a detailed analysis to form an ideal thermal cycle to model GSHP systems.

The total number of heating hours was calculated and then proportioned so that it could be distributed as shown in Figure 3. The total range of temperature that the soil would see was decided upon prior to the creation of the model. The energy pile's face reaches a maximum temperature of slightly more than 50 °C and a minimum temperature of slightly less than 0°C. The number of hours of heating was calculated using the method described above. The total number of heating hours was calculated to be 1,344 heating hours.

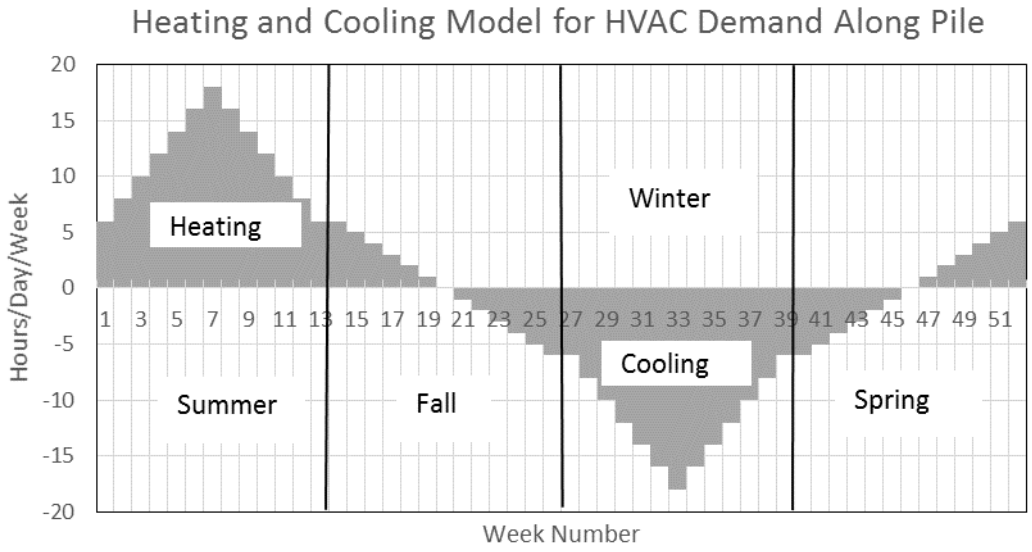

Figure 3. A chart modeling the seasonal heating and cooling demand used to model temperature change for the temperature boundary condition along the pile.

When heat is added to the energy pile, the pile undergoes volumetric strain. However, the vertical dimension may be ignored in order to find the effect the thermal expansion has upon the horizontal cross-sectional area of the pile and pile radius. The increase in the pile radius may result in increased total stress on the soil, in the form of increased u_e; the exception is the case of normally consolidated (NC) or slightly over-consolidated (OC) clays where the heating may cause thermal contraction of clay. The change in temperature between the in-situ temperature and the maximum soil temperature is 35°C. Using the modulus of elasticity and coefficient of thermal expansion for concrete presented above and Equation (13), the pile radius will expand 0.000076105 m during a change in temperature of 35°C. Using Equation (13) for a linear, compressive stress-strain relationship and assuming that since the stiffness of the concrete is much greater than that of the clay, the entirety of the strain from the thermal expansion of the energy pile is assumed to be transferred to the clay. The strain, ε, caused by the thermal expansion of the energy pile, represented by the right-hand side of Equation (13), is equal to the strain due to the linear compression of the clay, represented by $\frac{\sigma}{E_s}$ in Equation (13). This assumes that first, the clay does not undergo any volume change due to heating, and the confining around the pile does not constrain the radial expansion of the pile, which may not be true in the case of NC or slightly OC clays where thermal contraction occurs.

$$\varepsilon = \frac{\sigma R_{clay}}{E_s} = R_{pile}\alpha_c \Delta T \qquad (\mathbf{13})$$

where it is assumed that the radius of the energy pile, R_{pile}, is equal to the length of clay being compressed, R_{clay}. Assuming that the stress created by the thermal expansion of the energy pile is then equal to the strain multiplied by the modulus of elasticity of the clay, and that also assuming

that the stress, σ, is equal to an increase in the u_e, the u_e created by a temperature increase of 1 °C is calculated using Equation (14).

$$u_{heat} = \frac{\varepsilon E_s}{\Delta T} = \frac{(7.6105 \times 10^{-5})20{,}000\ kN/m^2}{35℃} = 0.0435\ \frac{kN}{m^2 \cdot ℃} \quad (\mathbf{14})$$

At this point in the model, the 182-day "construction phase" is over, and the model starts calculating the temperature change to the pile-soil boundary.

The value of u_{heat} in Equation (14) is multiplied by the change in the temperature calculated for that day to obtain the amount of the u_e caused by the thermal expansion of the pile. This temperature change is added to the previous temperature, and the density and coefficient of thermal expansion values of water are then recalculated. At this point, the model starts to account for the changes to the soil characteristics caused by the change in the temperature that was not required during the "construction phase" because the temperature was constant. The model then recalculates the minor changes in the density of the soil, $\rho_{clay,}$ and $\rho_{satclay}$. The specific heat is, thereafter, recalculated. The incremental temperature added to the previous day's temperature is then removed because the temperature is added to the previous day's temperature value in the part of the model that calculates conduction as a boundary condition along the pile face. This was necessary to prevent the change in temperature from being counted twice. Next, the u_e caused by thermal expansion of the soil is calculated. The values of the dynamic viscosity and thermal expansion of water are then calculated, which are in turn used to calculate the hydraulic conductivity and coefficient of consolidation. The u_e is thus calculated for the day, and then the values of the u_e caused by thermal expansion of the pile and thermal expansion of the soil are added. This totals the u_e value for the day. The unit-circumference skin friction is then calculated and recorded, and the time value advances afterward.

SUMMARY OF RESULTS

Figures 4 and 5 present the u_e data along the pile face at various depths. Figure 4 shows that the u_e at various depths experiences an initial rise in the value of approximately 14% immediately after pile installation. During this period, u_e values increase before consolidation begins—a dilatory response of the soil that is similar to that described in Burns and Mayne (1999). The u_e decreases more rapidly around Day 200. This coincides with the beginning of soil heating. The increased soil temperature increases the hydraulic conductivity of the soil. Another reason for this can be the thermally-induced water flow since water flows from hot to cold regions. To examine the contribution of this, the change in PWP at points at a distance from the energy piles need to be examined.

There is a small schematic image of the model to the left of each figure with a thick solid line marking the locations for which the results in the figure are shown. With the exception of the 15m case, other depths roughly coincide.

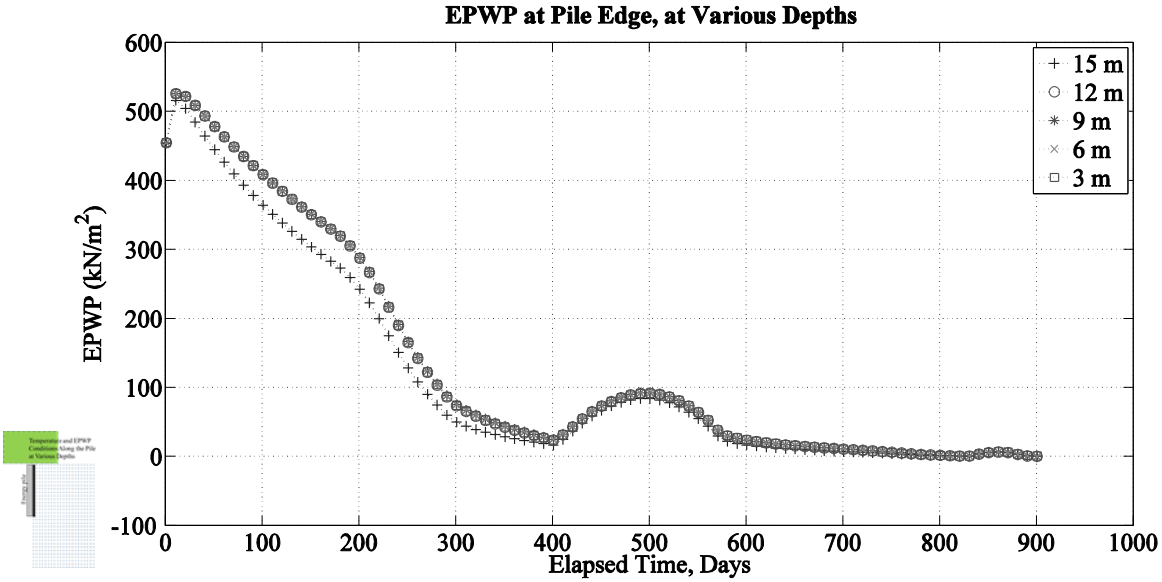

Figure 4. Excess pore-water pressure (EPWP, u_e) at the pile surface at various depths, from the time of pile installation to the end of the model run. The ground-surface temperature is a constant 15 °C.

On Day 402, and peaking on Day 497, the u_e increases 67 kN/m^2. This increase coincides with soil cooling during the winter season. There is another smaller increase in the u_e toward the end of Year 2. Figure 4 also shows that u_e values are almost equal along the pile face, with the exception of the 15m depth. This difference is likely due to the proximity of soil that has not undergone deformation due to cavity expansion within the assumptions of the model. In Figure 5 (the more realistic case with a transient ground-surface temperature), the influence of the ground-surface temperature has caused greater separation of the u_e values at the 3m depth from the values at the other depths.

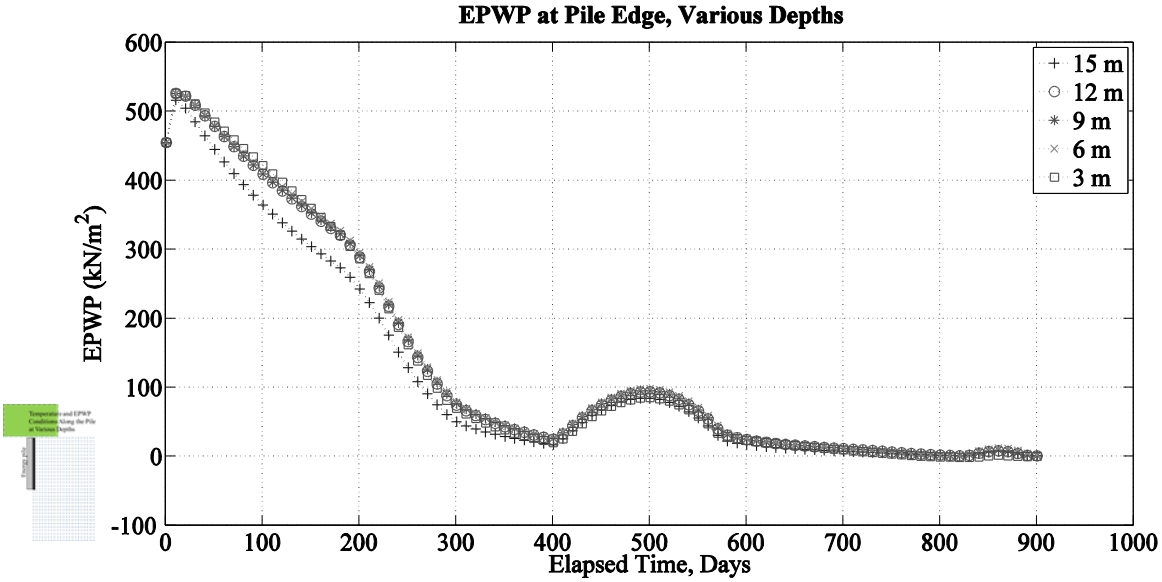

Figure 5. EPWP, u_e, at the pile surface at various depths.1, from the time of pile installation to the end of the model run, with transient ground-surface temperatures.

Results are available for other parameters at other locations at the same series of depths, which show more variations along the depth. However, those do not fit within the scope and limits of this paper.

The unit-circumference friction values are presented in Figures 6 and 7. Friction values drop after Day 1 until approximately Day 10, then rise until approximately Day 400, and thereafter decrease due to the increased u_e. The initial decreased friction values coincide with the period of dilation in the soil, where the u_e values rise for a period of time before decreasing. Friction values drop slightly again due to soil heating during the spring of Year 2. Unit-circumference-friction values are slightly higher in Figure 7 due to higher ground-surface temperatures. Although the friction capacity continues to increase until the end of the model run, the recommended unit-radius friction value is the value observed at the local minimum caused by soil cooling near the end of the first year of HVAC usage.

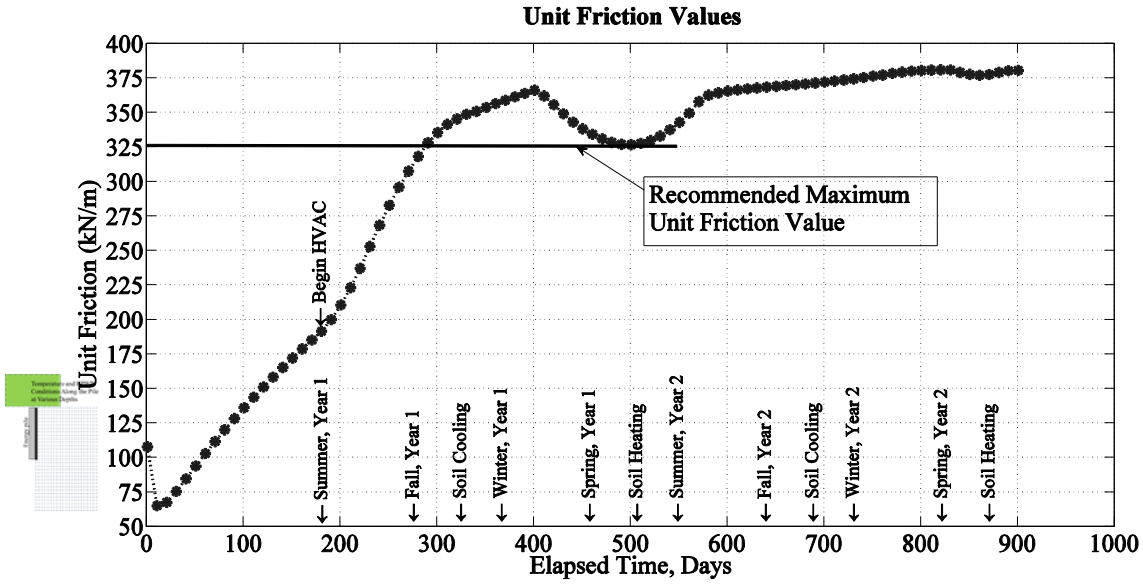

Figure 6. Unit-circumference-friction values from the time of pile installation to the end of the model run. The ground-surface temperature is a constant 15 °C.

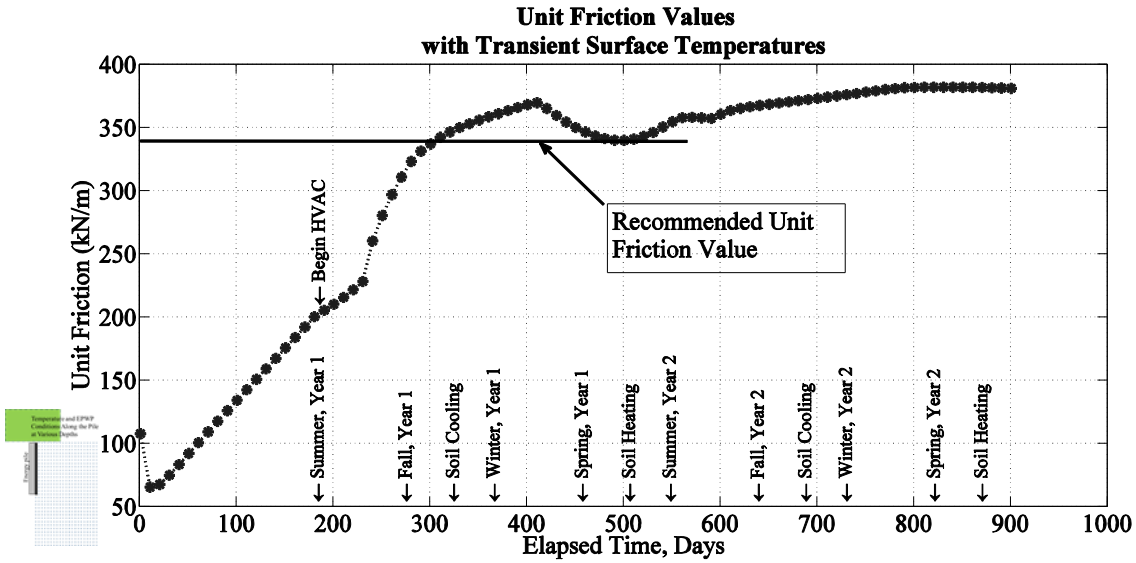

Figure 7. Unit-circumference-friction values from the time of pile installation to the end of the model run, with transient ground-surface temperatures.

CONCLUSION

The purpose of this paper was to understand the soil-pile interaction of energy piles and to model the effects of temperature fluctuation on the capacity of a driven energy pile in clayey soils. The involved physical processes include the consolidation of clay around energy piles as well as conduction through the saturated clay soil. The consolidation of clay (due to the drainage of the excess pore-water pressure, u_e, in clay) surrounding the energy pile affects the capacity of the pile (i.e., pile setup in clay). This work simulates how temperature fluctuations within the soil surrounding the energy pile and fluctuations of the ground-surface temperature affect the drainage of u_e and thus the capacity of the energy pile.

The change in the u_e due to the thermal expansion and contraction of the energy pile and thermal expansion and contraction of the soil matrix was included in the model as well as the dissipation of the u_e generated by cavity expansion during pile driving.

The model analyzed the effect that variable temperatures had on the capacity of driven energy piles. The temperatures of both the soil at the surface of the pile and the ground surface were varied sinusoidally to simulate seasonal demands on the energy pile and seasonal temperature changes, respectively.

The model assumed that the pile was driven on the first day of winter and the energy pile began operation on the first day of summer. The u_e dissipated at an increased rate during the period of time when the soil was heating. If the model conditions were flipped, i.e., the energy pile was constructed on the first day of summer and operational on the first day of winter, the u_e values would dissipate more slowly, likely leading to a longer period of consolidation and pile setup.

The influence of cyclical surface temperatures was observed in the results of the model. The offset in the cyclical surface-temperature equation placed the highest surface temperature in the middle of the summer, thus exaggerating the influence higher temperatures have on increasing consolidation rates because additional heat is present at the surface and is being conducted down into the soil at the same time the soil is heating due to HVAC usage. Consolidation rates would likely decrease more slowly if surface soil temperatures peaked during the period prior to operation of the energy pile and during the period of soil cooling.

The unit-circumference-friction values computed by the model were calculated where the effective vertical stress was calculated along the depth. The unit-circumference-frictional values computed in the model shown to lead to allowable side-friction-capacity values that were similar in value to the allowable capacities that were calculated, where the effective vertical stress was calculated as a single full-depth clay layer.

REFERENCES

Abdelaziz, S. L. (2016) *A Sustainable perspective for the long-term behavior of energy pile groups*. in *Geo-Chicago 2016*. 2016. Chicago, IL: ASCE.

Abdelaziz, S.L., Olgun, C. G., and Martin, J. R. (2015). *Equivalent energy wave for long-term analysis of ground-coupled heat exchangers.* Geothermics, **53**(1): p. 67-84.

Abdelaziz, S. L. (2015). *Deep Energy Foundations: Geotechnical Challenges and Design Considerations*. Ph.D. Thesis, *The Charles E. Via Department of Civil and Environmental Engineering*. 2013, Virginia Polytechnic Institute and State University. p. 368.

Abdelaziz, S.L. (2010). A Sustainable perspective for the long-term behavior of energy pile groups, *Proceedings of ASCE Geo-Chicago 2016*. 2016. Chicago, IL: ASCE.

Brandl, H. (2006). *Energy foundations and other thermo-active ground structures.* Geotechnique, 2006. **56**(2): p. 81-122.

Brandl, H. (2009). *Energy Pile Concepts. Deep Foundations on Bored and Auger Piles*, 77-95.

Burns, S., and Mayne, P. (1999). "Pore Pressure Dissipation Behavior Surrounding Driven Piles and Cone Penetrometers," *Transportation Research Record*, 1675, 17-23.

Campanella, R. G. and Mitchell, J.K. (1968). "Influence of Temperature Variations on Soil Behavior." ASCE *Journal of the Soil Mechanics and Foundations Division*, **94**(3), 709-734.

Coduto, D. (2001). *Foundation Design: Principles and Practices*, Second Edition. Prentice Hall. 402-558.

Holtz, B., Kovacs, W. D., and Sheahan, T. C. (2011) *An introduction to geotechnical engineering*, Prentice Hall, NJ.

Laloui, L., Nuth, M., and Vulliet, L. (2006). "Experimental and Numerical Investigations of the Behavior of a Heat Exchanger Pile." *International Journal of Numerical and Analytical Methods in Geomechanics*, **30**, 763-781.

McCartney, J. S. and Rosenberg, J. E. (2011). "Impact of Heat Exchange on Side Shear in Thermo-Active Foundations," ASCE *Geotechnical Special Publication, 211,* 488-498.

Mirza, U. A. A. (2000). "Consolidation Parameters from Axial Pile Load Tests." *Proceedings of The Tenth (2000), International Offshore and Polar Engineering Conference,* 395-402.

Ng, K., Roling, M., AbdelSalam, S., Suleiman, M., and Sritharan, S. (2013). "Pile Setup in Cohesive Soil. I: Experimental Investigation." *ASCE Journal of Geotechnical and Geoenvironmental Engineering.* **139**(2), 199-209.

Steward, E. J. and Wang, X. (2011). "Predicting Pile Setup (Freeze): A new approach considering soil aging and pore pressure dissipation." *ASCE Geotechnical Special Publication,* 211, 11-19.

Trachenko, K. (2008) "The Vogel–Fulcher–Tammann law in the elastic theory of glass transition." *Journal of Non-Cryst Solids,* 354, 3093–3906.

Wang, X., Verma, N., Tsai, C., and Zhang, Z. (2010). "Setup Prediction of Piles Driven into Louisiana Soft Clays." ASCE *GeoFlorida 2010 Conference: Advances in Analysis, Modeling & Design,* ASCE *Geotechnical Special Publication,* 199, 1573-1582.

Yang, L. and Liang, R. (2006). "Incorporating Set-up into Reliability-Based Design of Driven Piles in Clay." *Canadian Geotechnical Journal,* **43**(9), 946-955.